

Optimum Design of a Three-Phase Permanent Magnet Synchronous Motor for industrial applications

M.J. Soleimani Keshayeh*, S. Asghar Gholamian

Received: 6 June 2012 ; **Accepted:** 18 September 2012

Abstract Permanent Magnet Synchronous Motors (PMSMs) have been widely used in many industrial applications. In This paper a new method for multi objective optimal design of a permanent magnet synchronous motor (PMSMs) with surface mounted permanent magnet rotor is presented to achieve maximum efficiency and power density using a Bees algorithm for industrial applications. The objective function is a combination of power density and efficiency to be maximized simultaneously. A particular optimal machine is chosen and its performances are validated with FE analysis. The design optimization results in a motor with great improvement regarding the original motor.

Keywords Permanent Magnet Synchronous Motors, Design Steps, Bees Algorithm, Finite Element Analysis.

1 Introduction

Permanent magnet synchronous motors are a good choice in so many applications. Replacing excitation winding of rotor with permanent magnets (PM) makes these motors more efficient than their excited counterparts; hence they are used in applications with high efficiency. The most important advantages of such motors are: high efficiency and power density, low loss, low maintenance cost and etc [1,2,3,4].

Main application of permanent magnet synchronous motor (PMSMs) is aerospace, a traction motor for fuel cell electric vehicle, hybrid electric vehicle and automatic production systems in the industry.

Most of the time, these machines are used at steady-state and rated values. Hence, high efficiency is a frequent requirement [5]. Speed of synchronous motors can be accurately controlled by varying the frequency of the rotating magnetic field which is called synchronous speed. The permanent magnet synchronous motor eliminates the use of slip rings for field excitation, resulting in low maintenance and low losses in the rotor.

Hence, design optimization can enhance operational characteristics of motors.

Generally, the design and construction a PMSM must consider both of the stator and rotor structures in order to obtain a high performance motor. The stator windings are similar

* Corresponding Author. (✉)

E-mail: soleimani@stu.nit.ac.ir (M. J. Soleimani Keshayeh)

M. J. Soleimani Keshayeh

M.Sc. Student, Faculty of Electrical and Computer Engineering, Babol University of Technology, Babol, Iran.

S. Asghar Gholamian

Assistance Professor, Faculty of Electrical and Computer Engineering, Babol University of Technology, Babol, Iran.

to those in a poly phase ac motor, and the rotor is composed of one or more permanent magnets [5].

To go further in the rationalization of the design, an optimal design procedure can be adopted. Such a method, explained in [6, 7], several features of the machine. It has been successfully involved in the design of SMPMSM [8,9], and using analytical models [9,10,11], circuit type models [10] or finite-element (FE) models [8,12,13]. Jang et al [14] have used an analytical method to design a BLDC motor and validated the results by finite element method.

A GA-based optimal design of a high speed IPMSM has been proposed [15], considering efficiency as the objective function and motor weight as the constraints.

In this paper, a novel optimum design based on Bees algorithm (BA) is presented. The goal function in this paper is optimizing combination of power density and efficiency. In the following, it presents results of optimized PMSM motor.

The rest of the paper is organized as follow: section 2 explains design process. Section 3 presents the multi objective optimization design. Section 4 demonstrates optimization results and in section 5 simulation results of FEA are presented and based on results of the FEM calculation of the magnetic field, a comparison of the basic motor model and the BA solution is performed. Finally, the paper is concluded in section 6.

2 Design Steps of PMSMs

The permanent magnet AC motor, acting as conventional synchronous type motor, has found renewed interest in the last two decades [16, 17]. Fig.1 shows slot geometry for motor topology.

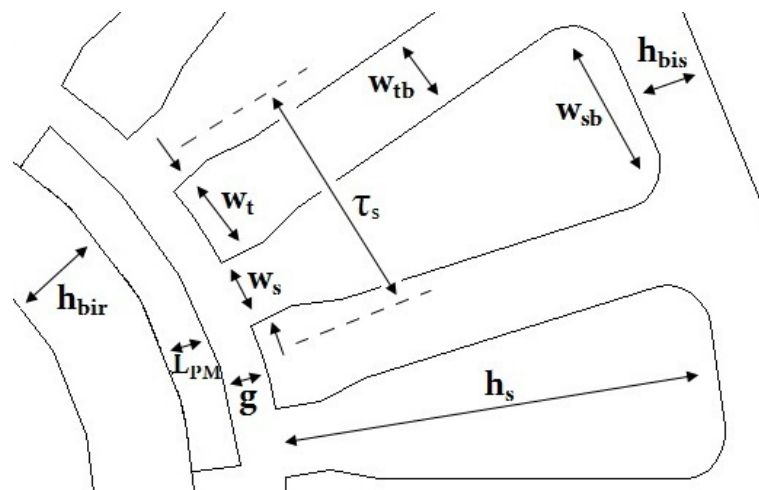


Fig.1 Motor topology showing geometrical definitions

Like all machine types, PMSMs are designed through some steps. These steps are categorized separately as follows:

2.1 The Parameters of PMSM

In this step, motor's main rated values are specified. In other word, ratings for a special application are chosen. The specification and geometry of the motor are shown in Table1 [18].

Table 1 Specification and Geometry of the motor

Designation	Unit	Value
Power	(kW)	1
Rated voltage	(V)	220
Rated speed	(rpm)	1500
Frequency	(Hz)	50
Number of pole	-	4
Number of slot	-	36

2.2 Determining the Materials Using of Motor

The development of the permanent magnet materials began in the early 20th century, first with magnetic steel [19]. In the 1930's the first material was developed which was useful for electro-mechanical devices. This was an aluminum-nickel-cobalt alloy AlNiCo which is still used in special applications but with decreasing importance. Its major drawback is a low coercive force H_c .

The next milestone in advances of permanent magnetism was the development of sintered rare-earth cobalt magnets around 1970, in particular samarium-cobalt alloys SmCo. However, the high price of the raw materials has prohibited a large scale use.

nowadays well known, NdFeB magnets, introduced in 1983. Although cheaper than SmCo and of even higher energy density, NdFeB is not always superior due to its lower thermal stability, caused by the lower Curie temperature, and its reactivity which leads for instance to corrosion problems.

What all these magnets have in common is the low permeability, similar to air. The relative permeability for NdFeB magnets is typically about $\mu_r = 1.05$.

For this motor, stator and rotor are composed of steel 100^a which B-H curve of that is shown in Fig.2.

Surface permanent magnets are NdFe35 with:

Br: 1.23 T,

Hc: 890 kA/m.

Whole-layer copper windings are embedded in 36 slots of the motor.

2.3 Winding of the AC Machines

Winding described here are those of stators of synchronous and asynchronous machines, or of wound rotor of asynchronous machines [20]. They are intended to create, when one feeds them by a system of three-phase currents, a rotating magnetic field.

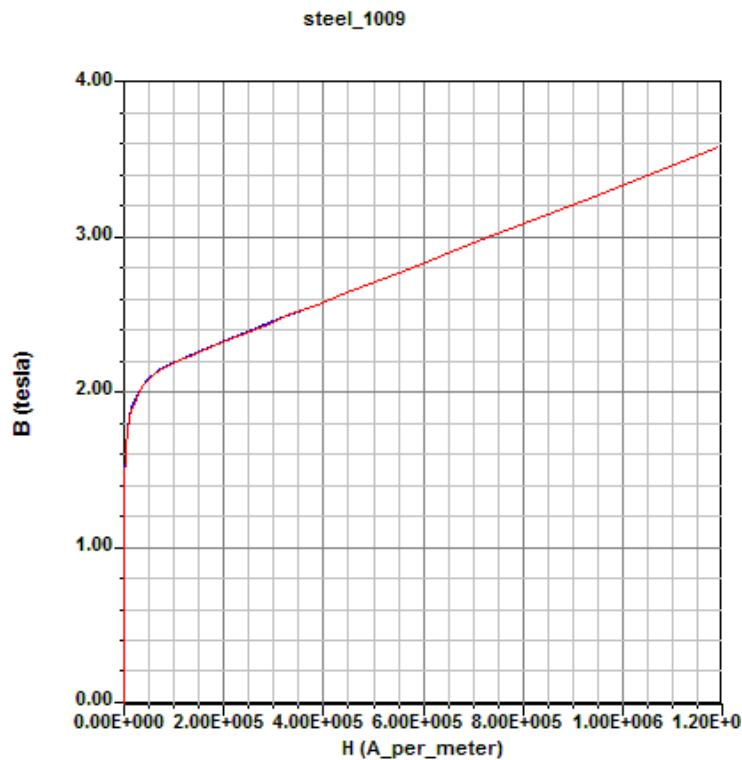


Fig.2 B-H curve of steel used for FEA

2.4 Design Variables

Designing electrical machines is highly concerned with machine's crucial variables. Proper selection of these variables leads to a good design. There are lists of variables in publications. Some of the most important ones with their constraints for PMSMs are listed in Table 2.

Normally, designer can chose a proper value between the limits by his experience or in some cases there are some tables which can help deciding the appropriate value. Generally speaking, these variables are selected based on motor's fundamental parameters introduced in Table 1.

Table 2 Motor's initial parameters

Variable	Description
B_{av} (T)	Specific magnetic loading
a_c (A/m)	Specific electric loading
B_g (T)	Air gap flux density
B_{ys}, B_{yr} (T)	Stator and rotor yoke flux density
B_t (T)	Stator tooth flux density
η (%)	Efficiency
PF	Power factor
L/τ_p	Axial length to pole pitch ratio
B_r (T)	Residual flux density

Specific electric loading depends upon several variables such as power rating, speed, frequency, and voltage rating. For machines with a smaller number of poles, a small diameter, or a large pole pitch, a smaller value of a_c should be used. Similarly, in high-voltage machines requiring larger slot insulation, a_c must be smaller. For machines with a larger number of poles, low voltage, and low frequency, a_c may be increased by up to 20% [18]. Proper value of a_c for PMSMs is in the range of 8000 to 30000 A/m.

The average flux density B_{av} is limited primarily by saturation and core loss. For PMSMs, the proper value of B_{av} is between 0.45 to 0.8 T [1, 21].

Other parameters such as flux density in stator and rotor yoke and tooth are around 1 to 2 T and they are selected according to the material used as stator and rotor core. Residual flux density is determined by magnet type. Axial length to pole pitch ratio is a very important parameter which is concerned with the shape of the magnet. Its range is $0.6 < L/\tau_p < 0.7$ for non-salient pole and $1 < L/\tau_p < 3$ for salient pole machines.

2.5 Determining the Dimensions and Parameters of Motor

Figure 3 shows motor's main dimensions. In this Figure, L is motor's axial length and D is stator inside diameter. These two parameters are the most crucial and prior dimensions in machine design which other dimensions and parameters are highly depended with them. Identity of motor is somehow specified by determining these two dimensions. [18,22].

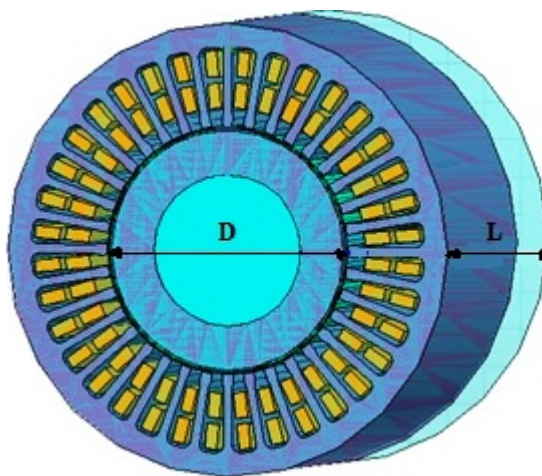


Fig. 3 Motor's main dimensions

2.5.1 Motor's Main Dimensions

Apparent input power is presented in (1)

$$Q = \frac{P_{out}}{\eta PF} kVA \quad (1)$$

Besides, this power can be rewritten in terms of motor's main dimensions

$$Q = C_0 D^2 L n_s \text{ KVA} \quad (2)$$

In electrical machine design, D^2L is an important parameter

$$D^2L = \frac{Q}{C_0 n_s} m^3 \quad (3)$$

where, Q is in KVA and n_s is rev/s.

By applying equation (3) and combining with (2), it is possible to obtain motor's main dimensions, i.e. L and D .

$$L = \alpha_\tau \frac{\pi D}{p} \quad (4)$$

where $\alpha_\tau = L/\tau_p$ and τ_p is in mm.

2.5.2 Air gap and Permanent magnet

Air gap of synchronous motors is determined by (5)

$$g = \gamma \tau_p \frac{ac}{B_\delta} \quad (5)$$

Magnet thickness is calculated as follow:

$$L_{PM} = (\mu_r B_g / (B_r - (K_f / K_d) B_g)) K_c g \quad (6)$$

where $k_f = B_{gpk}/B_g$ and k_d is leakage flux factor. Then, air gap of permanent magnet synchronous motors is calculated as follow

$$g_{PM} = L_{PM} / \mu_{rPM} + k_c g \quad (7)$$

It is recommended for small PMSMs to have $0.3 < L_{PM} < 1$ mm.

2.5.3 Conductor turn

Because of lamination of stator, stator has an effective axial length which is described as below:

$$L_i = L \times k_{st} \quad (8)$$

where k_{st} is stator stacking factor and is usually around 0.9. Flux under a pole is determined as follow :

$$\phi = B_{av} \cdot \tau_p \cdot L_i \quad (9)$$

Stator phase voltage is:

$$E_s = 0.97 \times V_L / \sqrt{3} \quad (10)$$

and number of phase turn of stator is calculated by

$$N_{ph} = \frac{E_s}{4.44 f \phi k_w} \quad (11)$$

Number of conductors in each slot is

$$Z_{slot} = \frac{6N_{ph}}{S} \quad (12)$$

2.5.4 Slot Dimensions

Determining slot dimensions is very important in design of electrical machines because it affects magnetic flux distribution and saturation. Hence, considerable efforts should be invested in this task.

Slot and PM configuration is shown in Figure 1 Parameters and dimensions are illustrated in this figure. Geometric parameters can be obtained through the parameters depicted in and Fig.4.

In this section, all the necessary dimensions of motor's slot are provided one by one.

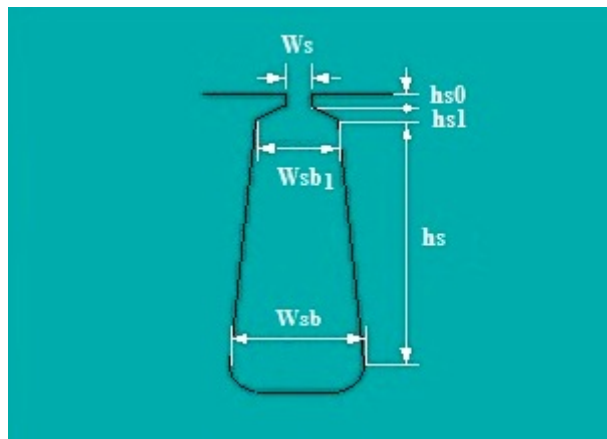


Fig. 4 Slot geometry for the radial-flux motor topology [from Maxwell13 software]

Slot pitch is the distance from the beginning of a slot to the beginning of the next one. It is formulated in (13) in mm.

$$\tau_s = \frac{\pi D}{S} \quad (13)$$

Maximum tooth width is

$$\omega_t = \frac{B_g \pi D}{B_t S} \quad (14)$$

Slot width is

$$\omega_s = \tau_s - \omega_t \quad (15)$$

Stator yoke height is

$$h_{bis} = \frac{B_g \pi D}{2B_{ys} p} \quad (16)$$

Similarly, rotor yoke height is [1]

$$h_{bir} = \frac{B_g \pi D}{2B_{yr} p} \quad (17)$$

Area in a slot can be found by below equation

$$A_{slot} = \frac{Z_{slot} I_s}{k_{fill} J_s} mm^2 \quad (18)$$

where k_{fill} has a value of 0.4 to 0.6.[2]

Initial slot depth is

$$h_s^{(1)} = \frac{A_{slot}}{\omega_s} \quad (19)$$

Slot bottom width, ω_{sb} , is calculated through following equation

$$\omega_{sb} + \omega_{tb} = \frac{\pi D_{sb}}{S} \quad (20)$$

Minimum tooth width is

$$\omega_{tb} = \frac{p\phi}{SB_t L_i} \quad (21)$$

Corrected slot depth is

$$h_s^{(2)} = A_{slot} / \left(\frac{\omega_{sb} + \omega_s}{2} \right) \quad (22)$$

2.6 Computation the Copper Losses and Iron Losses

High-speed rotation modifies the classical loss balance between iron and copper losses. Indeed, in classical rotational speeds the major part of losses corresponds to copper losses. However, when high rotational speed is considered, the iron losses and aerodynamic losses increase significantly and therefore are to be considered with particular attention.

In order to use the copper winding at best, the wire diameter must be chosen small enough to prevent penetration and proximity effects from being too important. Indeed, these effects are inevitable as soon as several wires are side by side and they make the copper losses increase. They can be neglected if the wire diameter is small enough compared to the depth of penetration, and if the wires are appropriately adjusted, like in Litz wire. These conditions are assumed to be satisfied in what follows.

From the equation of the copper losses (23):

$$P_{cu} = 3R_s(I_s)^2 \quad (23)$$

Phase current is

$$I_s = \frac{Q}{mE_s} \quad (24)$$

The phase resistance expression is given.

$$R_s = \frac{\rho \cdot T_s \cdot l_{mts}}{a_s \cdot 10^{-6}} \Omega \quad (25)$$

where $\rho = 1.8 \times 10^{-8}$ and $a_s = \frac{I_s}{J_s}$.

J_s is selected according to I_s . For small PMSMs, it has a value of 3 to 7 [1].

Core loss or iron loss is a form of energy loss which happens in electrical transformers and other inductors. High rotational speed involves high electrical frequency in the machine and leads to a consequent increase of iron losses in the magnetic paths [23]. For this reason high-speed machines tend to be designed with a low pole number [24] and with thin iron sheets, usually 0.35 or 0.2 mm.

Two types of iron loss are hysteresis loss and eddy current loss. The hysteresis is well known in ferromagnetic materials which the relationship between magnetic field strength (H) and magnetic flux density (B). The hysteresis loss results from the friction between the magnetic domain. Eddy current loss occurs when the rotating magnetic field induces

alternating current, called eddy current, in the iron core. The eddy current loss can be minimized by making the core with thin sheets or laminate sheets of magnetic material [25].

The iron losses can be determined by:

$$P_{iron} = K \times f_a \times |B|^\beta \times volume \quad (26)$$

3 Multi objective Optimization Design

The optimal design approach allows satisfying the specifications favoring some characteristics of the system.

Generally, optimization of a PMSMs motor is a multi-objective optimization problem with several variables and constraints. The optimization problem is defined through three steps.

First, the optimization variables, i.e. the motor geometric parameters, are defined. Second, the objective function and the constraints are formulated and finally an optimization solver is employed to find the optimal geometry of the motor.

The most crucial part of the optimization is the objective function formulation, which is normally a combination of power density, efficiency, power loss, cost and volume.

3.1 Optimization Problem

The designer is led to turn the design problem into an optimization problem constrained by restrictions over the research space as well as the solution space. For the targeted application, the machine can be designed for only multi operating point and it must develop 1 kW at 1500 r/min. A bi-objective optimization of efficiency (η) and power density (Pd) is carried out. The objective functions are computed as follows:

$$\eta = \frac{P_{out}}{P_{out} + P_{tot}} \quad (27)$$

$$P_{den} = \frac{P_{out}}{\frac{\pi}{4} D_o^2 L} \quad (W / m^3) \quad (28)$$

where D_o , is calculated through following equation (29)

$$D_o = D + 2h_s + 2h_{bis} \quad (29)$$

The geometric quantities can be seen in Fig.1. Among these design variables some are constrained to evolve within fixed ranges given in Table 3.

Table 3 optimization variable ranges

Quantity	Definition Range
motor axial length [mm]	[50 ; 150]
internal stator diameter [mm]	[50 ; 150]
external stator diameter [mm]	[100 ; 200]
Specific magnetic loading [T]	[0.45 ; 0.8]
Specific electric loading [A/m]	[8000 ; 30000]
Axial length to pole pitch ratio	[1 ; 3]
Power factor	0.8
AC voltage[v]	220

This optimization must satisfy the constraints expressed in Table 4.

3.2 Optimization Method

The electrical machine design optimization problem is complex. Moreover, the global optimum is researched. These particular features are well treated by BA [26].

3.2.1 Bees Algorithm

Swarm-based algorithms have well shown their efficiency in solving complex multi-variable optimization problems. Bees Algorithm (BA), proposed by Pham in 2005 [27], is a newly born swarm-based algorithm that mimics the food foraging behavior of swarms of honey bees. In this paper, BA is applied to find near-optimal values for PM synchronous motor parameters. This entails an optimization of multivariable functions. In what follows, first the nature-inspired foundation for BA is explained and then a description of the algorithm is depicted.

A colony of honey bees starts foraging by sending scout bees to perform a random search for promising food sources. The colony has the ability to explore long distances (about 14 km) in multiple directions, which assures exploiting a large number of patches [28,29]. As the foraging process advances, a number of bees in the colony are always assigned as scout bees [29]. If the food gathered from a patch meets a criterion threshold, the scout bee deposits it in the hive and advertises the relative patch in the waggle dance [28]. The waggle dance is an important means of communication in the colony and provides it with all the necessary information of the outside [28, 30]. The bees in the hive choose among different patches according to the information obtained from waggle dances about their relative qualities. Thus, more bees visit the more promising patches [30, 31], this helps an efficient foraging process. Recruiting more bees to a promising patch continues until the patch fitness is decided to fall below the criterion threshold. The Bees algorithm requires a number of parameters to be set, namely: number of scout bees (N), number of sites selected out of N visited sites (M), number of best sites out of M selected sites (E), number of bees recruited for best E sites (Nre), number of bees recruited for the other (M-E) selected sites (Nsp), the size of neighborhood search (ngh), and the stopping criterion.

The algorithm steps are depicted as below:

- (I) create an initial population randomly.

(II) Evaluate fitness of the initial population.

(III) Do the following steps.

1. Select sites for neighborhood search.
2. Recruit bees for selected sites and evaluate the goal function.
3. Select the best bee from each patch.
4. Perform random searches for remaining bees and evaluate their Fitnesses.
5. If the criterion is met, stop; otherwise go to step (III).

“Selected sites” which have the highest fitness are chosen in step 1 for neighborhood search. Searches in the neighborhood of the selected sites are performed in step 2 and step 3. Neighborhoods of the best E sites are searched more finely than the other selected sites i.e. more bees are recruited to them. This differential recruitment together with scouting, are the major feathers of the Bees Algorithm. In step 3, the fittest bee from each patch is selected to form the next bee population. The remaining bees are assigned to search randomly in step 4. These steps are repeated until a stopping criterion is met.

In this study, each bee represents six design parameters i.e.

motor axial length (L), internal stator diameter(D), external stator diameter (Do), Specific magnetic loading (B_{av}), Specific electric loading (ac), Axial length to pole pitch ratio(L/τ_p).

Other design parameters are obtained through equations described in section 2. The structure of the proposed method is illustrated through a flowchart in Fig.5.

BA is applied to optimize three goal functions: power density - output power per volume - (F1), efficiency which is output power divided by input power (F2), and the combination of the two first functions that is: $F=\beta_1F_1+\beta_2F_2$ where $\beta_1+\beta_2=1$. For each of these three functions, the optimal values are produced after various tunings of BA parameters.

The seven parameters of BA are categorized in four groups for tuning.

1. From the results N, E, M which determine the size of population.
2. Nre, Nsp which determine number of neighborhood patches to search
3. ngh which determines the size of neighborhood search.
4. Iteration which is the stopping criterion.

gained after tuning parameters of each group, it can be observed that the most efficient BA parameter values in terms of goal functions' optimal values, convergence of optimization process, and smoothness of output plot is as Table 4.

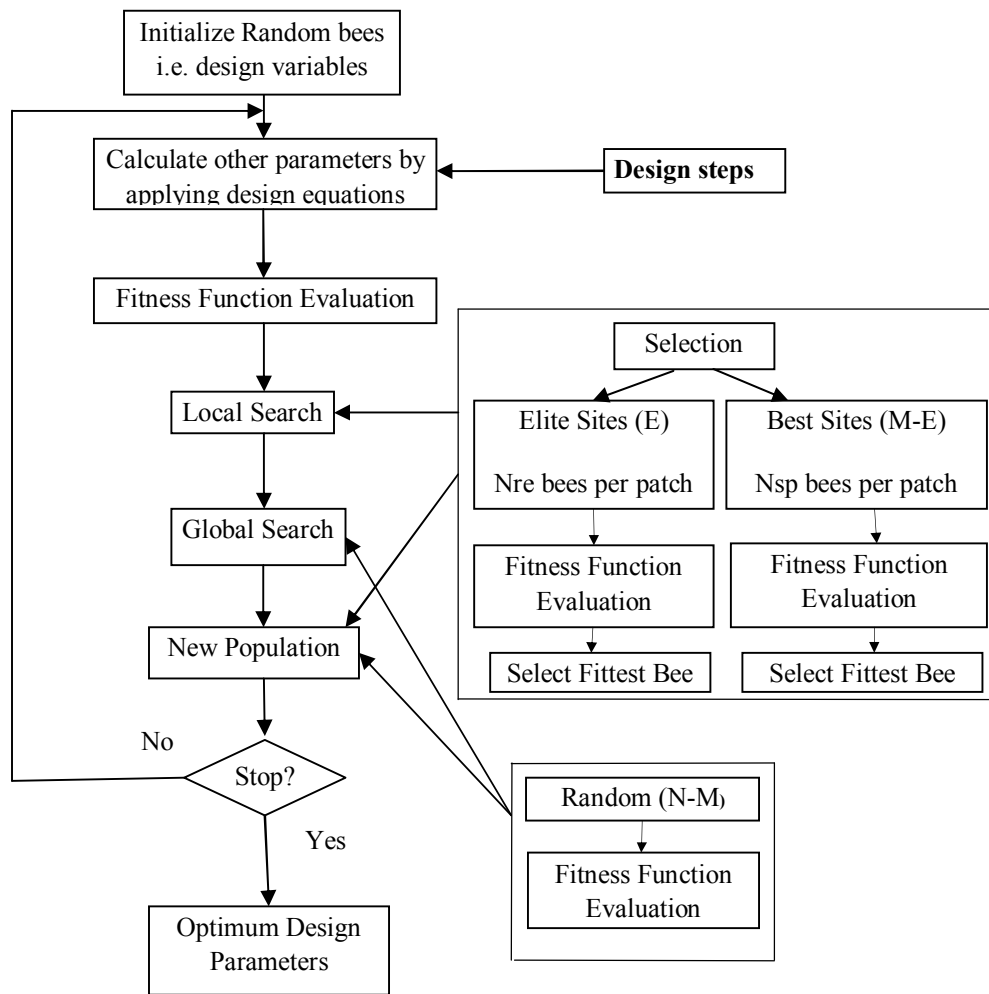


Fig. 5 structure of the proposed method

Table 4 BA parameters values

BA Parameters	Value
N	200
M	170
E	150
Nre	50
Nsp	30
Ngh	variable range/10000
Iteration	100

The effects caused by changing values of parameters in each group on output results can be described as follow:

- Population size (N, E, M) should be large enough to ensure convergence and smoothness of the output plot while it's too large amount is redundant.

- Neighborhood search size (ngh) value should be small enough so that the optimal value of goal function is found, while its too small amount may cause steps in output plot.
- Number of neighborhood patches (Nre, Nsp) should be large enough to ensure the convergence and smoothness of the output plot.
- Iteration number (iteration) should be large enough to ensure the convergence, while its too large amount is redundant.

4 Optimization Results

In this section, the results obtained from optimization of a PM synchronous motor parameters by the bees algorithm are presented. All simulations are done applying the MATLAB 2010 software. Nominal design parameters of this motor and related restriction are presented in table5.

Table 5 Nominal design parameters of motor

Design Parameters	Value
Voltage	220 V
Output power	1 KW
Number of poles	4
Number of phases	3
number of slots	36
Slot fill factor	0.5
Slot per Pole per Phase	2
flux density in stator	1.5 T
flux density in rotor	1.5 T
Residual flux density of PM	1.2 T

Figure6 shows power density unit (F1) versus iteration. The optimal value of power density is 1.81 (W/cm³).

Figure7 shows efficiency (F2) versus iteration. The optimal value of efficiency is 95.4. Figure8 shows combination of power density and efficiency (F) versus iteration. Dimensions of optimal PM synchronous motor is Shown in Table6.

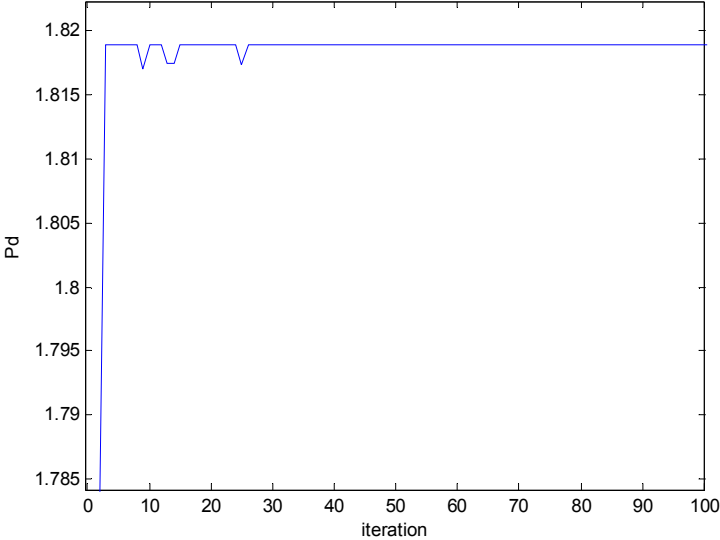


Fig. 6 power density unit (F1) versus iteration

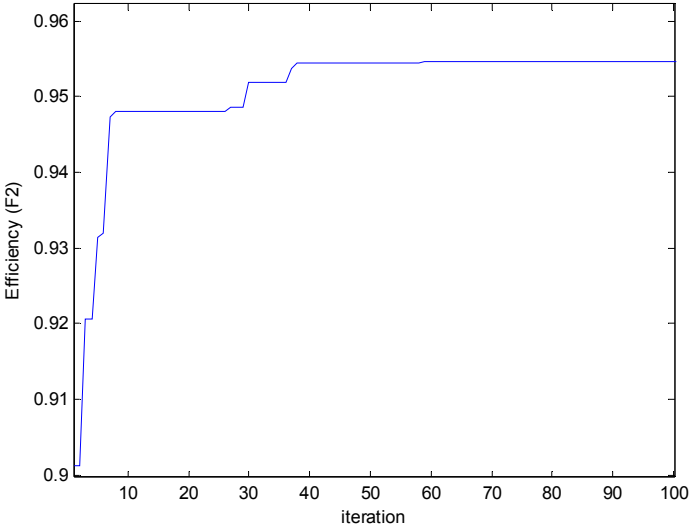


Fig. 7 efficiency (F2) versus iteration

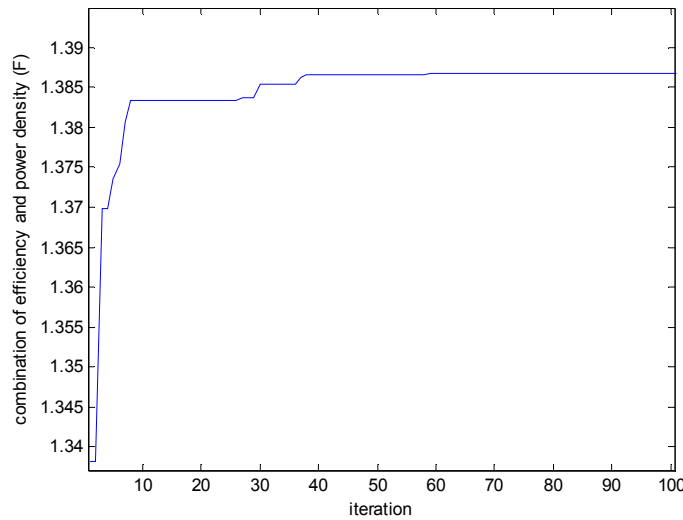


Fig 8 combination of power density and efficiency (F) versus iteration

Table 6 Dimensions of optimal PM synchronous motor

Design Parameters	Value
D (mm)	60
L (mm)	70
g (mm)	0.1
L_{pm} (mm)	0.31
τ_p (mm)	85
Φ (wb)	0.0015
τ_s (mm)	5.23
ω_t (mm)	2.7
ω_s (mm)	2.5
ω_{tb} (mm)	2.1
ω_{sb} (mm)	3.14
h_s (mm)	14.66
h_{bir} (mm)	12.56
Power density (W/cm ³)	1.81
Efficiency (%)	95.4

5 Finite Element Magnetic Method

The finite element method which found its way into electrical engineering almost 30 years ago, has long offered the tantalizing promise of providing us with a design tool that gives detailed information about the electromagnetic conditions within the heart of a motor. The advantage of numerical methods like the finite element method is that arbitrary shapes, arbitrary boundary conditions and complicated or distributed sources, can be used with essentially no extra effort [32].

Desirable output quantities can be extracted using this software. Design procedure of this program can be summarized as follow:

- Applying optimized dimension calculated by BA to the project

- Assigning materials and boundary to the project
- Performing mesh operation
- Setting up an analysis to solve
- Extracting output data and plots.

5.1 The Calculation Results

The software called Finite Element Magnetic Method (Maxwell2D) is used in the design calculation of the PM machine.

Fig. 9 shows the 2-D finite element mesh generated in the project. Fig.10 shows the flux density distribution in the motor which its maximum occurs in the corner of tooth. Flux lines diagram is shown in Fig. 11.

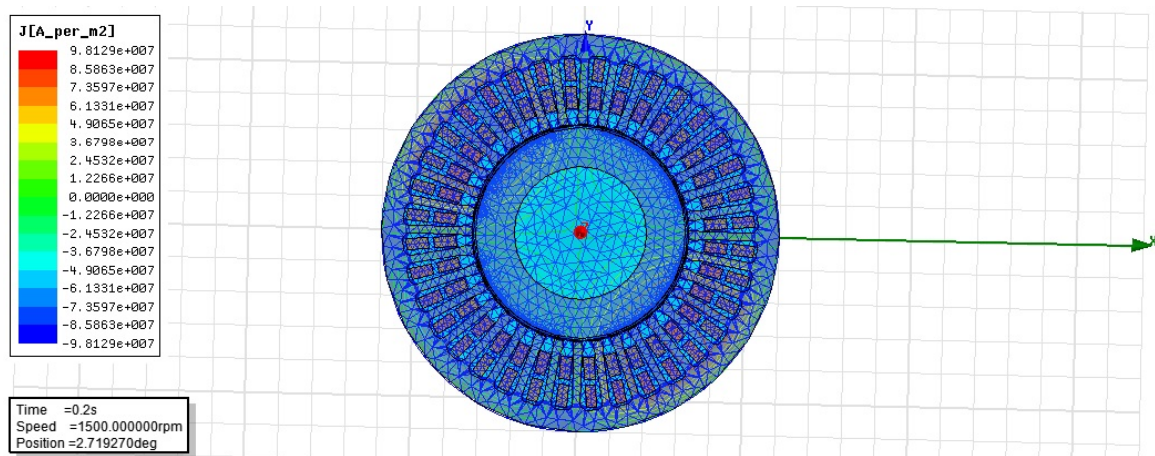


Fig. 9 Mesh diagram

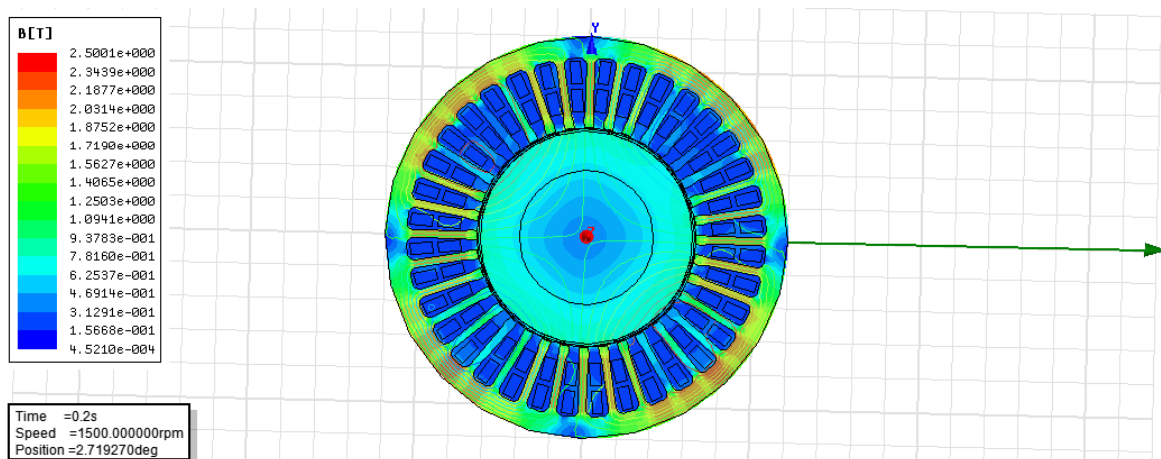


Fig. 10 Flux density distribution

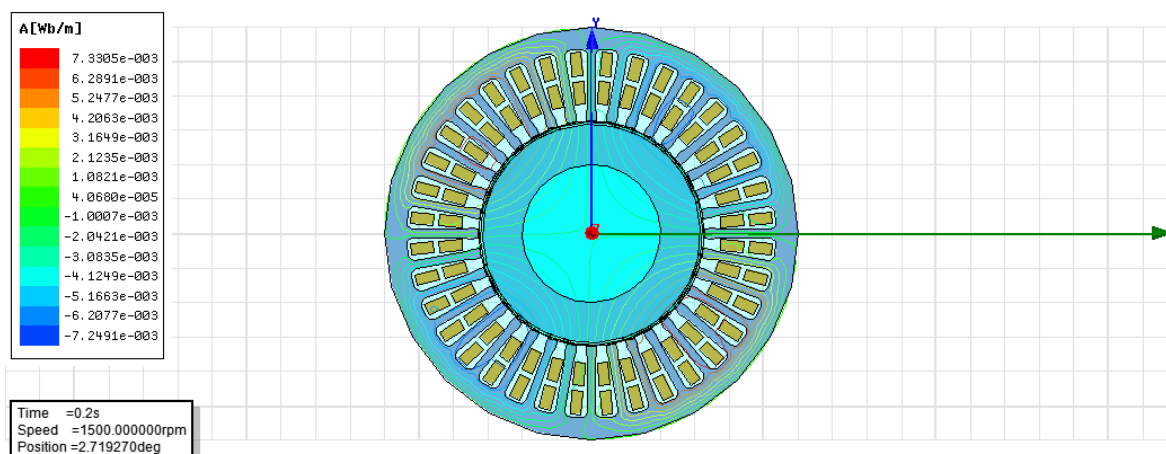


Fig. 11 Flux lines diagram

The analytically computed maximal magnetic flux density in the stator iron is 0.98 T. It is noted that the FE-computed relative permeability is constant everywhere in the machine, which validates the linear hypothesis made for the analytical model. The deviation between the analytical results and the FE computations are within a range of 10% which is acceptable for a first order analytical modeling.

After all, a comparison is done between analytical and numerical results in Table 7. In this table, flux density in stator and rotor are maximum value and in air gap is average. As shown, FEA validates optimization results properly.

Table 7 Analytical and Numerical results comparison

	B_{cs}	B_{cr}	B_{ag}
Analytical (T)	1.5	1.5	0.55
Numerical (T)	1.46	1.47	0.517
Error (%)	2.6	2	6

6 Conclusions

In this paper, a comprehensive formulation needed in optimal design of permanent magnet synchronous motors with surface magnet structure has been presented considering power density and efficiency. A novel optimal design of permanent magnet motor based on the bees algorithm (BA) is proposed. The aim of this work is to maximize three goal functions: power density, efficiency, and the combination of the two first functions.

Various tuning of BA parameters were considered for each of these three optimization processes. The best tuning is chosen in terms of goal functions' optimal values, convergence of optimization process, and smoothness of output plot.

Furthermore, this paper applies a 2-D finite Element program to validate the proposed algorithm. Simulation results confirm optimized data with a little degree of error. The results have been analyzed and showed the efficacy of the proposed technique.

Future work may be devoted to developing other goal functions which result in a more efficient optimization of motor design parameters. Other optimization methods such as artificial bee colony, particle swarm optimization, and genetic algorithm can be applied to the considered problem to the hope of achieving more optimal results.

References

1. Pyrhonen, J., Jokinen, T., Hrabovcova, V., (2008). Design of Rotating Electrical Machines. John Wiley & Sons.
2. Yeadon, W., Yeadon, A., (2001). Handbook of Small Electric Motors, McGraw-Hill Professional; 1 edition.
3. Melfi, M. J., Rogers, S. D., Evon, S., Martin, B., (2008). Permanent-magnet motors for energy savings in industrial applications. *IEEE Trans. Ind Appl.*, 44(5), 1360–1366.
4. Soleimani, M. J., ILka, R., Asghar Gholamian, S., (2011). Optimal design of permanent magnet brushless DC motor, PSC. [in Persian].
5. Hendershot, J. R., Miller, T. J. E., (2010). Design of Brushless Permanent-Magnet Machines. Publisher: Motor Design Books LLC, Second Edition.
6. Mester, V., Gillon, F., Brochet, P., Wurtz, F., (2008). Multimodel sizing for the optimal design of electric machines. Optimal design method. *Revue Int. Génie Electr.*, 11(6), 695–715.
7. Asghar Gholamian, S., ILka, R. Soleimani, M. J., (2011). Optimal design of Double sided axial flux permanent magnet motor using genetic algorithms. First Conference on New Approaches to Computer Engineering & IT. [in Persian].
8. Schatzer, C., Binder, A., (2000). Design optimization of a high-speed permanent magnet machine with the VEKOPT algorithm,” in Proc. Conf. Record 2000 IEEE Ind. Appl. Conf., 1, 439–444.
9. Ojo, O., (1991). Multiobjective optimum design of electrical machines for variable speed motor drives. in Proc. Conf. Record 1991 IEEE Ind. Appl. Soc. Annual Meet., 1, 163–168.
10. Markovic, M., Perriard, Y., (2009). Optimization design of a segmented Halbach permanent-magnet motor using an analytical model. *IEEE Trans. Magn.*, 45(7), 2955–2960.
11. Bianchi, N., Bolognani, S., Frare, P., (2006). Design Criteria for High-Efficiency SPM Synchronous Motors. *IEEE Transactions on energy conversion*, 21(2).
12. Kim, K. C., Lee, J., Kim, H. J., Koo, D. H., (2009). Multiobjective optimal design for interior permanent magnet synchronous motor. *IEEE Trans. Magn.*, 45(3), 1780–1783.
13. Islam, M. S., Islam, R., Sebastian, T., (2011). Experimental Verification of Design Techniques of Permanent-Magnet Synchronous Motors for Low-Torque-Ripple Applications. *IEEE Transactions On Industry Applications*, 47(1).
14. Jang, S. M., Cho, H. W., Choi, S. K., (2007). Design and analysis of a high-speed brushless DC motor for centrifugal compressor. *IEEE Transactions on Magnetics*, 43(6), 2573–2575.
15. Xavier Jannot, Jean-Claude Vannier, Claude Marchand, Mohamed Gabsi, Jacques Saint-Michel, Daniel Sadarnac, (2011). Multiphysic Modeling of a High-Speed Interior Permanent-Magnet Synchronous Machine for a Multiobjective Optimal Design. *IEEE Transactions On Energy Conversion*, 26(2).
16. Low, S., Lee, W. H., (1987). Characteristics and Performance Analysis of a Permanent Magnet motor with a Multistacked Imbricated Rotor. *IEEE Trans. on Energy Conversion*, EC-2(3), 450–457.
17. Petkovska, L., (1991). A Contribution to Analysis of Permanent Magnet Excitation Field Influence on Characteristics of an Electronically Operated Synchronous Motor, via 3D Magnetic Field Calculation. PhD Thesis, Skopje, Macedonia, 214.
18. Toliyat, H. A., Kilman, G. B., (2004). Handbook of Electric Motors, Second Edition. Taylor & Francis Group.
19. Eckart Nipp. (1999). Permanent Magnet Motor Drives with Switched Stator Windings. TRITA-EMD 9905 ISSN-1102-0172. Royal Institute of Technology Department of Electric Power Engineering Electrical Machines and Drives. Stockholm.
20. Takorabet, N., (2004). Materials Regional Workshop on Electrical Motor Design and Actuators. CODE 1A-005-00.
21. Hamdi, E. S., (1994). Design of Small Electrical Machines. John Wiley & Sons, ISBN-10: 0471952028.
22. Luo, S. H. J., Leonardi, F., Lipo, T. A., (1998). A General Approach to Sizing and Power Density Equations for Comparison of Electrical Machines. *IEEE Transactions on Industry Applications*, 34(1).

23. Binder, A., Schneider, T., (2008). High-speed inverter-fed AC drives. in Proc. 2007 Int. Aegean Conf. Electr. Mach. Power Electron. (ACEMP), 748–755.
24. Thelin, P., Nee, H. P., (1998). Suggestions regarding the pole-number of inverter-fed PM-synchronous motors with buried magnets. in Proc. 7th Int. Conf. Power Electron. Variable Speed Drives, London, U.K., 544–547.
25. Wikipedia Foundation Inc. (2006). Core loss, Eddy current, Hysteresis. Iron loss [serial online] [cited 2006 Oct 15].
26. Pham, D. T., Ghanbarzadeh, A., Koç, E., Otri, S., Rahim, S., Zaidi, M., The Bees Algorithm – A Novel Tool for Complex Optimisation Problems. Manufacturing Engineering Centre, Cardiff University, Cardiff CF24 3AA, UK.
27. Pham, D. T., Ghanbarzadeh, A., Koç, E., Otri, S., Rahim, S., Zaidi, M., The Bees Algorithm – A Novel Tool for Complex Optimisation Problems. Manufacturing Engineering Centre, Cardiff University, Cardiff CF24 3AA, UK.
28. Von Frisch, K., (1976). Bees: Their Vision, Chemical Senses and Language. (Revised edition) Cornell University Press, N.Y., Ithaca.
29. Seeley, T. D., (1996). The Wisdom of the Hive: The Social Physiology of Honey Bee Colonies. Massachusetts: Harvard University Press, Cambridge.
30. Camazine, S., Deneubourg, J., Franks, N. R., Sneyd, J., Theraula, G., Bonabeau, E., (2003). Self-Organization in Biological Systems. Princeton: Princeton University Press.
31. Bonabeau, E., Dorigo, M., Theraulaz, G., (1999). Swarm Intelligence: from Natural to Artificial Systems. Oxford University Press, New York.
32. Vahed Kalankesh, H., Sharifian, M. B. B., Feyzi, M. R., Multiobjective Optimization of Induction Motor Slot Design Using Finite Element Method. *Journal of Biotechnology*, 10(69), 15662-6.